

# Effect of external magnetic field on morphology and microstructure of wire arc additive manufacture

Honglei Zhao

Yiwen Li

Yajie Sun

Zhihai Dong

Huifang Liu

Aleksandr Babkin

Yunlong Chang (✉ [zh108302021@126.com](mailto:zh108302021@126.com))

Shenyang University of Technology

---

## Research Article

**Keywords:** WAAM, Magnetic field, Surface forming accuracy, Microstructure

**Posted Date:** March 29th, 2022

**DOI:** <https://doi.org/10.21203/rs.3.rs-1234284/v1>

**License:** © ⓘ This work is licensed under a Creative Commons Attribution 4.0 International License.

[Read Full License](#)

---

# Abstract

The longitudinal magnetic field assisted CMT+P process is used for arc fuse additive manufacturing of aluminum alloy. Analyze the forming and organization properties of additive components. The excitation frequency is 40Hz ~ 70Hz, and the excitation current is 4A ~ 8A, during the additive manufacturing process. The results show that the external magnetic field can improve the forming and organization properties of the material, but the size of the magnetic field has a reasonable matching interval. The optimal parameter is when the excitation frequency is 50Hz and the excitation current is 5A. The influence of the magnetic field promotes the flow process in the molten pool, increases the homogenization of alloying elements, reduces the temperature gradient and promotes the equiaxed crystallization and refinement of crystal grains. The surface tension of the molten pool is weakened under the action of an external magnetic field. The size and frequency of the magnetic field affect the stability of the molten pool flow and the crystallization of the molten pool.

## 1. Introduction

The material utilization rate is not high in the traditional manufacturing process, because the parts are generally made by cutting, milling and other methods. Herranz et al. [1] used traditional milling methods to manufacture aircraft structural parts and found that the material utilization rate was only 5%. Therefore, the method of additive manufacturing is proposed. Wire + Arc Additive Manufacturing (WAAM) has attracted attention because of its higher efficiency compared with other additive methods. Traditional cold metal transition (CMT) technology used in additive manufacturing is prone to porosity. Cong et al. [2] used the CMT Pulse (CMT+P) process to add aluminum alloy and significantly reduce the porosity of the component. However, when the CMT+P process is used for adding materials, the forming accuracy of the parts still cannot meet the requirements, and the organization and performance still need to be optimized and improved. Song et al. [3] combined the advantages of addition and subtraction and adopted the "3D welding and milling" method to improve the surface accuracy of parts. Yin et al. [4] obtained the regression equation based on the quadratic regression rotation combination test, which can effectively predict the width of the cladding layer. Martina et al. [5] used a high-pressure interlayer rolling and feeding method to convert the columnar crystals of the transverse members into 56-139 micron equiaxed crystals. Asala et al. [6] used post-deposition heat treatment (PDHT) to treat additive components to eliminate softening and analyze performance from a microstructure perspective.

The external magnetic field can control the arc shape and the droplet transition process, control the metal flow in the molten pool, and have a good performance on the forming and microstructure properties of the parts. Takeda et al. [7] studied the time response of an arc driven by an external magnetic field, and obtained arc plasma trajectories under different magnetic field parameters. Chang et al. [8] applied an appropriate magnetic field to increase the droplet transfer frequency of gas metal arc welding (GMAW) and reduce spatter. Luo et al. [9] improved the droplet transfer process of carbon dioxide gas shielded welding (CO<sub>2</sub> welding) by increasing the longitudinal magnetic field, reduced spatter, and obtained a uniform and refined weld microstructure. Liu et al. [10] significantly improved the structure and properties

of aluminum alloys by using alternating magnetic field aging treatment. Zhu et al. [11] studied the changes of microstructure and mechanical properties with excitation current. Therefore, based on the CMT+P method and the longitudinal magnetic field, it is of great significance to study the influence of the magnetic field on the surface forming and microstructure properties of WAAM parts.

## 2. Material And Experiments

### 2.1 Material and equipments

The experiment uses  $\Phi$  1.2mm ER2319 Al-Cu aluminum alloy welding wire for additive processing. The alloy composition of this material is shown in Table 1 below. The additive manufacturing system is shown in Fig. 1. The additive manufacturing process is implemented using Fronius CMT (A-4600) welding machine and wire feeder (marked 1 in Fig. 1) and ABB robot (marked 2 in Fig. 1) in CMT+P mode. The magnetic field is introduced by the magnetic field generator (marked 3 in Fig. 1) and the excitation power supply MCWE-40/2000 (marked 4 in Fig. 1). The additive process takes place on the workbench (marked 5 in Fig. 1). Each machine is cooled by a water tank (marked 6 in Fig. 1). OLYMPUS type metallographic microscope is used to observe the metallographic structure of the sample after welding.

| Si   | Fe   | Cu    | Mn    | Mg   | Zn   | Ti    | Zr    | Al      |
|------|------|-------|-------|------|------|-------|-------|---------|
| 0.20 | 0.30 | 5.80- | 0.20- | 0.02 | 0.10 | 0.10- | 0.10- | Balance |
|      |      | 6.80  | 0.40  |      |      | 0.20  | 0.25  |         |

Table 1 Alloy composition of ER2319 (wt.%)

### 2.2 Experiment method

The thickness of the component is measured with an ultrasonic thickness gauge with an accuracy of 0.01mm. The specific operation is as follows: select the surface of one side of the component as the measurement object, and divide it into n 1cm·1cm grids. Take a point in each grid and measure the thickness of each point with an ultrasonic thickness gauge. Calculate the variance of the thickness  $h_i$  and the average thickness  $\bar{h}$  at n different positions. The surface flatness formula is shown in formula 1.

$$Pa = \frac{1}{n} \sum_{i=1}^n (h_i - \bar{h})^2 \quad \text{Formula 1}$$

Where: "Pa" is the surface flatness, "n" is the number of measuring points, "hi" is the thickness of the i-th measuring point, and " $\bar{h}$ " is the average thickness of n measuring points. The smaller the "Pa", the better

the surface flatness of the component, and the smoother the surface of the component, the better the forming effect. The larger the "n" value, the more accurate the surface flatness characterization.

## 3. Results And Discussions

### 3.1 The influence of external magnetic field on the morphology

#### 3.1.1 The influence of different excitation frequencies on morphology

When the excitation current is constant (5A), the excitation frequency ( $E_f$ ) is 40-70Hz, and the component morphology which under the influence of magnetic field (MF) is shown in Fig. 2.

The outer wall of the component is relatively flat without the influence of the magnetic field, but the stacking width inside the component is not consistent (Fig. 2 (a) red box). The shape of the component gets better and then worse as the  $E_f$  increases. Compared with the absence of a magnetic field, the surface unevenness is optimized at  $E_f = 40\text{Hz}$ . The surface of the element is smooth at  $E_f = 50\text{Hz}$ . when  $E_f = 60\text{ Hz}$  and  $E_f = 70\text{ Hz}$ , the surface of the part flows and even collapses, which seriously affects the forming accuracy.

The wall thickness of the component is measured with an ultrasonic thickness gauge, and the surface flatness of the component under each  $E_f$  is calculated, as shown in Fig. 3.

The thickness of the outer wall is more stable after the external magnetic field is applied. The outer wall becomes more uniform as the  $E_f$  increases. Among them, the characteristic parameter with the smallest fluctuation is  $E_f = 50\text{Hz}$ . When  $E_f = 70\text{Hz}$ , the thickness has a large range of fluctuations, showing defects of macroscopic morphology.

For the above phenomenon, we believe that it is mainly caused by the interaction of the surface tension ( $F_s$ ), the magnetic field force ( $F_m$ ) and the induced current ( $I_i$ ) generated in the molten pool. M. O. et al. [12] established a welding pool model for simulation analysis and found that the metal flow on the surface of the weld pool is mainly affected by  $F_s$ .  $F_s$  is reflected in the molten pool as the viscous force on the surface of the molten pool. The decrease of  $F_s$  will weaken the viscous force on the surface of the molten pool, which is easy to cause the molten pool to flow outward. In the absence of a magnetic field,  $F_s$  plays a leading role in the flow of the molten pool. Heat accumulation easily occurs in the arc additive process. Since  $F_s$  will gradually decrease with the increase of temperature, it will cause uneven wall thickness of the additive component and poor molding quality. After applying a magnetic field, as  $E_f$  increases: the inductive reactance in the magnetic field generator gradually increases, so  $F_m$  will gradually decrease;  $I_i$  gradually increases, so the Joule heat generated in the molten pool gradually increases, and  $F_s$  will gradually decrease.

When the excitation frequency is low ( $E_f = 40\text{Hz}$ ),  $F_m$  is large, which plays a leading role in the flow of the molten pool, and  $F_s$  is relatively small. The molten pool metal flows under the restriction of  $F_m$ . Compared with the non-magnetic field, the shape of the component becomes better. However, because the  $F_m$  is too large, the flow velocity of the molten pool is too fast and unstable, and the optimization effect of component forming is not outstanding. When the excitation frequency is moderate ( $E_f = 50\text{Hz}$ ),  $F_m$  is relatively reduced, and  $F_s$  is further reduced.  $F_m$  still plays a leading role in the flow of the molten pool. Because of the moderate  $F_m$ , the flow of the molten pool is slow and stable, and the components are formed well. When the excitation frequency is high ( $E_f = 60\text{Hz}-E_f = 70\text{Hz}$ ),  $F_m$  is further reduced and  $F_s$  is further reduced. At this time, because  $F_m$  is too small, the flow of the molten pool cannot be effectively restricted, and  $F_s$  is also reduced too much. Therefore, the viscosity of the molten pool drops and flows around.

### **3.1.2 The influence of different excitation current on morphology**

When the excitation frequency is constant (50Hz), the excitation current ( $E_c$ ) is 4-8A, and the component morphology which under the influence of magnetic field (MF) is shown in Fig. 4.

The forming quality of the component is good first and then bad as the excitation current increases. When  $E_c=4\text{A}$ , the surface of the component is uneven, and the forming quality is not as good as when there is no magnetic field. When  $E_c=5\text{A}$ , the surface of the part is smooth and the forming quality is relatively best. The phenomenon of surface flow appears as the excitation current continues to increase. When  $E_c=8\text{A}$ , the surface of the component collapses, and the quality of component forming is poor.

Surface flatness under excitation current is shown in Fig. 5.

The thickness of the outer wall is more stable after the external magnetic field is applied. The outer wall becomes more uniform as  $E_c$  increases. The characteristic parameter with the smallest fluctuation is  $E_c = 5\text{A}$ . When  $E_c = 8\text{A}$ , the thickness has a large range of fluctuations, showing defects of macroscopic morphology.

In the absence of a magnetic field,  $F_s$  plays a leading role in the flow of the molten pool. After applying a magnetic field, as  $E_c$  increases:  $F_m$  will gradually increase and  $I_l$  will gradually increase, so the Joule heat generated in the molten pool will gradually increase, and  $F_s$  will gradually decrease.

When the excitation current is small ( $E_c = 4\text{A}$ ),  $F_m$  is small and  $F_s$  is relatively large, which plays a leading role in the flow of the molten pool. Therefore, similar to the absence of a magnetic field, the component forming changes are not obvious. When the excitation current is moderate ( $E_c = 5\text{A}$ ),  $F_m$  is relatively increased, and  $F_s$  is relatively decreased.  $F_m$  plays a leading role in the flow of the molten pool. Because of the moderate  $F_m$ , the flow of the molten pool is slow and stable, and the components are formed well. When the excitation current is large ( $E_c = 6\text{A} - E_c = 8\text{A}$ ),  $F_m$  increases further and  $F_s$  decreases further.  $F_m$

still plays a leading role in the flow of the molten pool, but the molten pool flow is too fast and unstable due to the large  $F_m$ , resulting in poor forming of the component.

## **3.2 The influence of external magnetic field on microstructure**

### **3.2.1 Effect of excitation frequency on microstructure**

From the microstructure diagram shown in Fig. 6, it can be found that the external magnetic field plays an important role in the crystallization and solidification process.

The overall microstructure of the component is layered in the absence of a magnetic field. It is mainly composed of small equiaxed crystals and columnar crystals. When  $E_f = 40\text{Hz}$ , due to the small electromagnetic stirring effect, the microstructure changes little. When  $E_f=50\text{Hz}$ , the coarse columnar crystals are almost completely transformed into fine equiaxed crystals, and the crystal grains become smaller and uniform. As the excitation frequency continues to increase ( $E_f=60\text{Hz}-E_f=70\text{Hz}$ ), directional columnar and dendritic crystals are formed.

### **3.2.2 Effect of excitation current on microstructure**

The influence of different excitation current on microstructure is shown in Fig. 7.

There are obvious coarse and fine grain regions in the microstructure. When  $E_c=5\text{A}$ , the structure is almost completely transformed into fine equiaxed crystals, and the grain refinement effect is the most obvious. The grains gradually coarsened with the increase of  $E_c$ . When  $E_c=6\text{A}$ , the equiaxed crystal is coarse. When  $E_c=7\text{A}$ , the crystal grains grow directionally to form columnar crystals. When  $E_c=8\text{A}$ , the solidified structure is composed of coarse columnar crystals and columnar dendrites.

## **3.3 The influence of external magnetic field on mechanical properties**

In order to more quantitatively reflect the influence of the magnetic field, tensile tests and hardness tests were carried out on the components. According to the experimental data, the influence of the magnetic field parameters on the mechanical properties of the additive components is analyzed.

### **3.3.1 Influence of excitation frequency on mechanical properties**

The mechanical properties of parts under different  $E_f$  is shown in Fig. 8. The green line is the component elongation (%), which corresponds to the green axis on the right side of the figure. The remaining parameters correspond to the left axis.

The hardness of the component is the maximum at the wall, followed by the "+" shape, and then the "T" shape, and the minimum at the corner. Calculate the difference between the maximum and minimum hardness of the component under different excitation frequencies. It can be obtained that the component hardness difference is 4.58 HV when there is no magnetic field. When  $E_f = 50\text{Hz}$ , the component hardness difference is the smallest, which is 3.09 HV. The hardness of each part of the component is more uniform under this parameter.

As the excitation frequency increases, the tensile properties of the component increase first and then decrease. When  $E_f = 50\text{Hz}$ , the tensile strength, yield strength and elongation of the component are relatively highest. Compared with no magnetic field, the tensile strength is increased by 10%, the yield strength is increased by 4%, and the elongation is increased by 5.56%.

### **3.3.2 Influence of different excitation current on mechanical properties**

The mechanical properties of components under different  $E_c$  is shown in Fig. 9.

When  $E_c = 5\text{A}$ , the hardness difference of each part of the component is the smallest, and the hardness of each part of the component is uniform.

As  $E_c$  increases, the tensile properties of the element first increase and then decrease. When  $E_c = 5\text{A}$ , the tensile strength, yield strength and elongation of the component are relatively high.

### **3.4 Effect mechanism of external magnetic field on structure properties**

The change of WAAM composition under the action of the external magnetic field mentioned above is caused by the crystallization and solidification process of the molten pool under the action of the magnetic field, as shown in Fig. 10. Due to the external magnetic field, an induced current ( $I_i$ ) appears in the high temperature molten pool.  $I_i$  will drive the melt to move, and the direction of movement depends on the direction of the magnetic field.

When no magnetic field is applied, the stratification of the component microstructure is mainly affected by two aspects: (1) The stratification of the two adjacent stacked layers. During the additive process, the welding starting points of the two adjacent stacked layers are not on the same vertical line. At the beginning of welding the first layer, due to the low substrate temperature, the rapid cooling makes the molten pool easy to form finer equiaxed crystals. However, with the input of heat, the rapid cooling effect disappears, the heat dissipation conditions are poor, and the crystal grains become coarse; when the second layer is welded after cooling, the welding starting point is not above the welding starting point of the first layer, but above the first layer with coarse grains. Therefore, the phenomenon of organization delamination of two adjacent accumulation layers is produced. (2) Single-layer organization

stratification. The rapid cooling of the bottom of the single-layer molten pool forms equiaxed crystals. The crystals in the middle of the molten pool grow along the direction of the maximum temperature gradient. Since the heat flow direction diffuses in the stacking direction perpendicular to the substrate, the columnar crystal grains grow in the direction perpendicular to the substrate. As a result, delamination of single-layer columnar crystals and equiaxed crystals occurs.

After the magnetic field is applied, the stirring force generated by the magnetic field will continue to destroy the semi-solidified grains. Damaged crystal grains form more nucleation bases, the number of crystal grains increases, and the crystal grains are refined. The excitation frequency and excitation current have different influence rules on the crystallization of the molten pool. As the excitation frequency increases ( $E_f=40\text{Hz}$ - $E_f=70\text{Hz}$ ),  $F_m$  gradually decreases,  $I$  gradually increases, and the electromagnetic damping effect in the molten pool increases. When  $E_f=40\text{Hz}$ ,  $F_m$  is larger, and the molten pool flows under the action of a larger magnetic field. However, due to the low stirring frequency of the molten pool, the grain refinement effect is not obvious. Compared with the case without a magnetic field, the structure and performance of the component are no different. When  $E_f=50\text{Hz}$ , the magnetic field force is moderate, the frequency is moderate, the stirring effect of the molten pool is good, the crystal grains are almost all refined, and good structure and performance are obtained. When  $E_f=60\text{Hz}$  and  $E_f=70\text{Hz}$ ,  $F_m$  is smaller and stirring force is smaller. Due to the large electromagnetic damping effect in the molten pool, the growth of crystal grains is promoted, resulting in coarse crystal grains and poor structural performance of the components. As the excitation current increases ( $E_c=4\text{A}$ - $E_c=8\text{A}$ ),  $F_m$  gradually increases. When  $E_c=4\text{A}$ ,  $F_m$  is small, the stirring effect of the molten pool is not obvious, and the structure and performance of the components are not much different from those without magnetic field. When  $E_c=5\text{A}$ , the  $F_m$  is moderate, the stirring effect of the molten pool is good, and good organizational properties are obtained. When  $E_c=6\text{A}$ - $E_c=8\text{A}$ ,  $F_m$  is large, which makes the molten pool stirring unstable, uneven temperature field distribution in the molten pool, and poor component structure and performance.

The driving force has a greater influence on the bottom of the molten pool than it is close to the surface of the molten pool. The alloy elements at the bottom of the molten pool are transported to the weld zone through the movement of the melt, which increases the uniformity of the alloy element distribution in the weld zone. The flow of the molten pool reduces the temperature gradient in the weld zone and reduces the possibility of columnar crystal formation. In addition, the movement of the molten pool will increase the squeezing force between the semi-solidified grains, so the equiaxed crystal ratio increases, and the width of the fine equiaxed crystal region increases.

## 4. Conclusion

By applying an external magnetic field to the WAAM process and adjusting the appropriate  $E_f$  and  $E_c$ , the magnetic field strength matching the additive process can be obtained, and a good macroscopic appearance can be obtained. Through experimental comparison, the following conclusions are drawn:

1. The results show that the external magnetic field has a certain restrictive effect on the flow of the molten pool. Within a certain range of magnetic field strength and frequency, the organization and performance of the material are improved. When  $E_f = 50\text{Hz}$  and  $E_c = 5\text{A}$ , the magnetic field strength and frequency of the magnetic field have a relatively stable influence on the WAAM process, and the material has the best tensile strength and yield strength. As  $E_f$  and  $E_c$  continue to increase, the tensile strength and yield strength of the material decrease.  $E_f$  and  $E_c$  have different influences on the flow of the molten pool.
2. The influence of the magnetic field promotes the flow process and electromagnetic stirring in the molten pool, increases the homogenization of alloy elements, reduces the temperature gradient, and promotes the equiaxed crystallization and refinement of crystal grains. The variation range of the maximum and minimum hardness difference of each part of the additive component is smaller, and the hardness distribution is more uniform.
3. Under the action of an external magnetic field, the surface tension of the molten pool is weakened, and the stability of the flow of the molten pool and the crystallization of the molten pool are mainly related to the size and frequency of the magnetic field.

## **Declarations**

### **Ethical Approval**

We comply with the COPE guidelines and make the following commitments. All the data and experimental contents involved in this manuscript are original. It does not involve publishing in any form or language elsewhere. The quoted words of other people are marked in the text by reference.

### **Consent to Participate**

All co-authors are aware of the writing and publication of this article and agree to publish it.

### **Consent to Publish**

All co-authors agree to publish this article.

### **Authors Contributions**

All co-authors participated in the writing or guidance of the paper and played an important role.

## Funding

The present research work was financially supported by Key Research and Development Project of Liaoning Province [Grant No. 2019JH2/10100017], Special project for the transformation of major scientific and technological achievements in Shenyang (Grant No. 20-203-5-01), the National Natural Science Foundation of China (Grant No. 51775354), Liaoning Revitalization Talents Program (Grant No. XLYC2007072) and the Ministry of Education and Science of Russian Federation (Grant No.11.9505.2017/8.9).

## Competing Interests

The authors declare that they have no known competing financial interests or personal relationships that could have appeared to influence the work reported in this paper.

## Availability of data and materials

All data in this manuscript is original and does not involve any copyright issues.

## Acknowledgements

The present research work was financially supported by Key Research and Development Project of Liaoning Province [Grant No. 2019JH2/10100017], Special project for the transformation of major scientific and technological achievements in Shenyang (Grant No. 20-203-5-01), the National Natural Science Foundation of China (Grant No. 51775354), Liaoning Revitalization Talents Program (Grant No. XLYC2007072) and the Ministry of Education and Science of Russian Federation (Grant No.11.9505.2017/8.9).

## References

1. Herranz S, Campa FJ, de Lacalle LN, López, Rivero A, Lamikiz A, Sánchez J, Bravo A (2005) U., The milling of airframe components with low rigidity: A general approach to avoid static and dynamic problems. *Proceedings of the Institution of Mechanical Engineers, Part B: Journal of Engineering Manufacture.* 219(11), 789-802. doi: 10.1243/095440505X32742
2. Cong BQ, Ding JL, Williams S (2015) Effect of arc mode in cold metal transfer process on porosity of additively manufactured Al-6.3%Cu alloy. *The International Journal of Advanced Manufacturing Technology* 76(9–12):1593–1606. doi: 10.1007/s00170-014-6346-x
3. Song YA, Park S, Choi D, Jee H (2005) 3d welding and milling: part i-a direct approach for freeform fabrication of metallic prototypes. *International Journal of Machine Tools & Manufacture* 45(9):1057–1062. doi: 10.1016/j.ijmachtools.2004.11.021

4. Yin F, Wang K, Feng Y, Luo T (2018) Machine Building & Automation 47(3):119–122. doi: 10.19344/j.cnki.issn1671-5276.2018.03.029. Width dimension modeling and analysis of wire and arc additive manufacture
5. Martina F, Colegrove PA, Williams SW, Meyer J (2015) Microstructure of interpass rolled wire + arc additive manufacturing ti-6al-4v components. Metallurgical & Materials Transactions A 46(12):6103–6118. doi: 10.1007/s11661-015-3172-1
6. Asala G, Khan AK, Andersson J, Ojo OA (2017) Microstructural analyses of ati 718plus produced by wire-arc additive manufacturing process. Metallurgical & Materials Transactions A 48(9):4211–4228. doi: 10.1007/s11661-017-4162-2
7. Takeda K, Okubo H, Sugimoto M (2014), Time response of arc driven by alternating magnetic field. Journal of Physics: Conference Series. 550, 012011. doi: 10.1088/1742-6596/550/1/012011
8. Chang YL, Liu XL, Lu L, Babkin AS, Lee BY, Gao F (2014) Impacts of external longitudinal magnetic field on arc plasma and droplet during short-circuit gmaw. International Journal of Advanced Manufacturing Technology 70(9–12):1543–1553. doi: 10.1007/s00170-013-5403-1
9. Luo J, Luo Q, Wang XX, Wang XC (2010) EMS-CO<sub>2</sub> Welding: A New Approach to Improve Droplet Transfer Characteristics and Welding Formation. Mater Manuf Processes 25(11):1233–1241. doi: 10.1080/10426914.2010.481000
10. Liu YZ, Zhan LH, Ma QQ, Ma ZY, Huang MH (2015) Effects of alternating magnetic field aged on microstructure and mechanical properties of aa2219 aluminum alloy. J Alloys Compd 647. doi: 10.1016/j.jallcom.2015.05.183
11. Zhu S, Wang QW, Wang XM, Han GF (2011) Analysis on thermal efficiency and softening behavior of mig welding with longitudinal magnetic field. Adv Mater Res 148–149:326–331. doi: 10.4028/www.scientific.net/AMR.148-149.326
12. Mo CL, Geng XW, Zhou XH, Cong R (2014), Simulation of the tig melt pool of 2a16 aluminum alloy. Journal of Shenyang Aerospace University. 31(03), 45-48. doi: CNKI: SUN: HKGX.0.2014-03-009

## Figures

### Figure 1

Additive manufacturing system



(a) Without MF

(b)  $E_f = 40\text{Hz}$

(c)  $E_f = 50\text{Hz}$



(d)  $E_f = 60\text{Hz}$



(e)  $E_f = 70\text{Hz}$

**Figure 2**

Morphology of WAAM components (a) Without MF, (b) With MF ( $E_f = 40\text{Hz}$ ) , (c) With MF ( $E_f = 50\text{Hz}$ ) , (d) With MF ( $E_f = 60\text{Hz}$ ) , (e) With MF ( $E_f = 70\text{Hz}$ )

**Figure 3**

Flatness of component surface at different  $E_f$

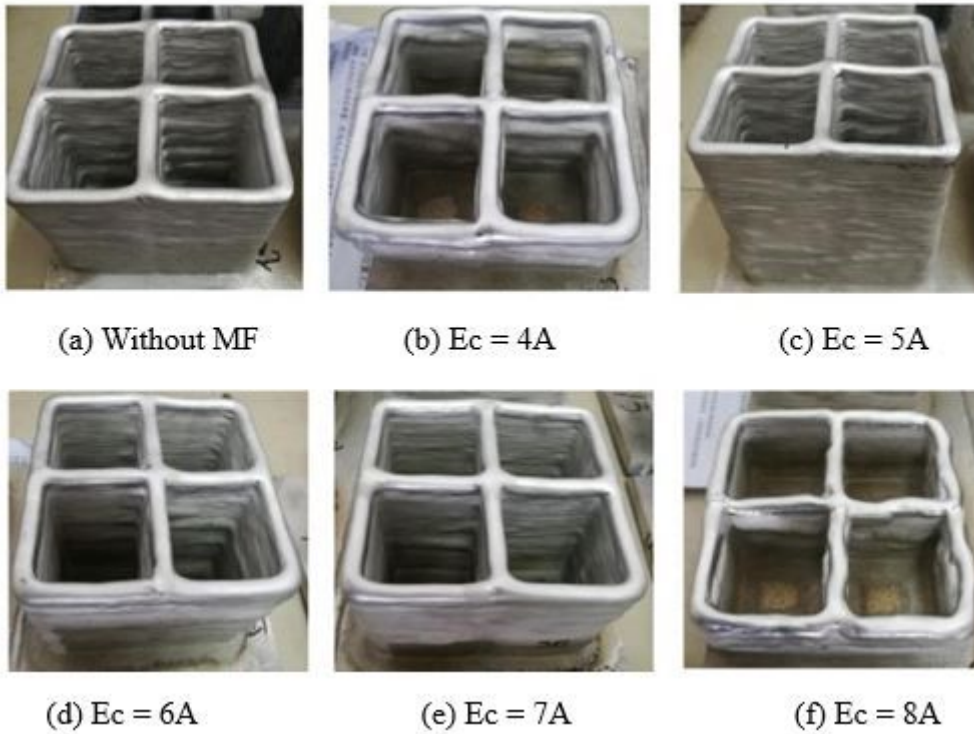


**Figure 4**

Morphology of WAAM components (a) Without MF, (b) With MF ( $E_c = 4A$ ) , (c) With MF ( $E_c = 5A$ ) , (d) With MF ( $E_c = 6A$ ) , (e) With MF ( $E_c = 7A$ ) , (f) With MF ( $E_c = 8A$ )

**Figure 5**

Flatness of component surface at different  $E_c$

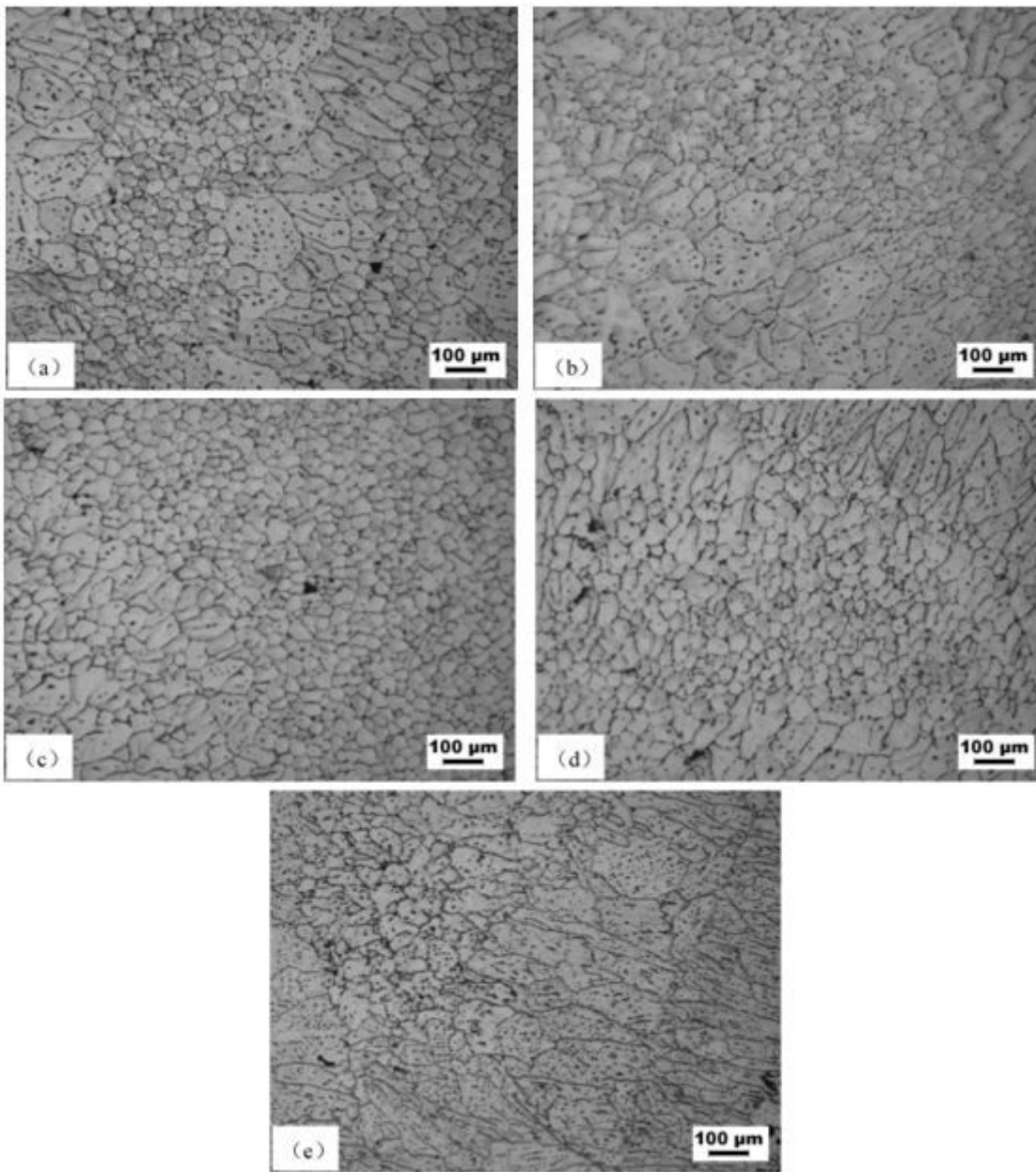


**Figure 6**

Influence of excitation frequency variation on microstructure (a) Without MF, (b) With MF ( $E_f = 40\text{Hz}$ ), (c) With MF ( $E_f = 50\text{Hz}$ ), (d) With MF ( $E_f = 60\text{Hz}$ ), (e) With MF ( $E_f = 70\text{Hz}$ )

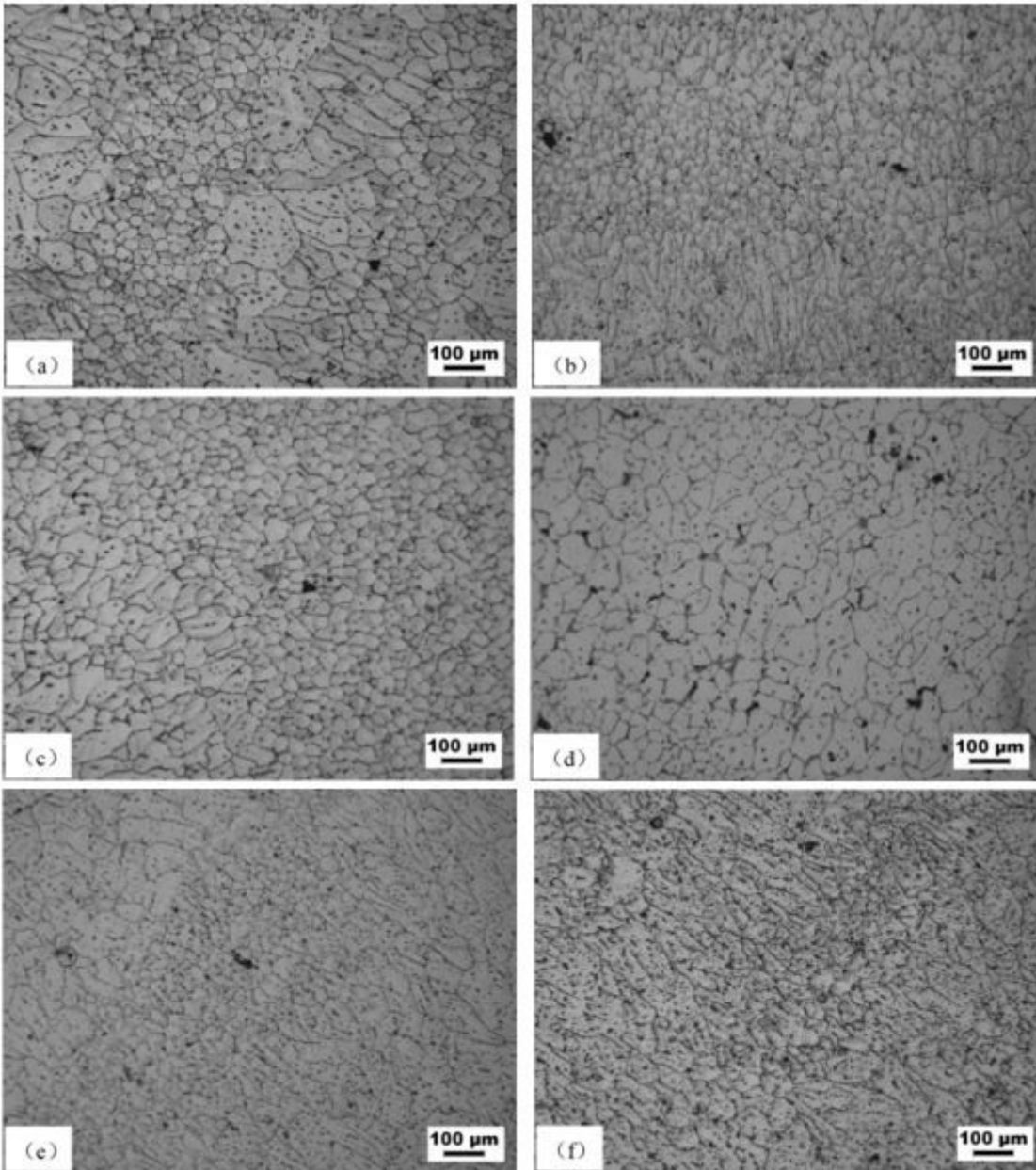


**Figure 7**

Influence of excitation current variation on microstructure (a) Without MF, (b) With MF ( $E_c = 4A$ ) , (c) With MF ( $E_c = 5A$ ) , (d) With MF ( $E_c = 6A$ ) , (e) With MF ( $E_c = 7A$ ) , (f) With MF ( $E_c = 8A$ )



**Figure 8**

Mechanical properties of components under different excitation frequencies



**Figure 9**

Mechanical properties of components under different excitation currents

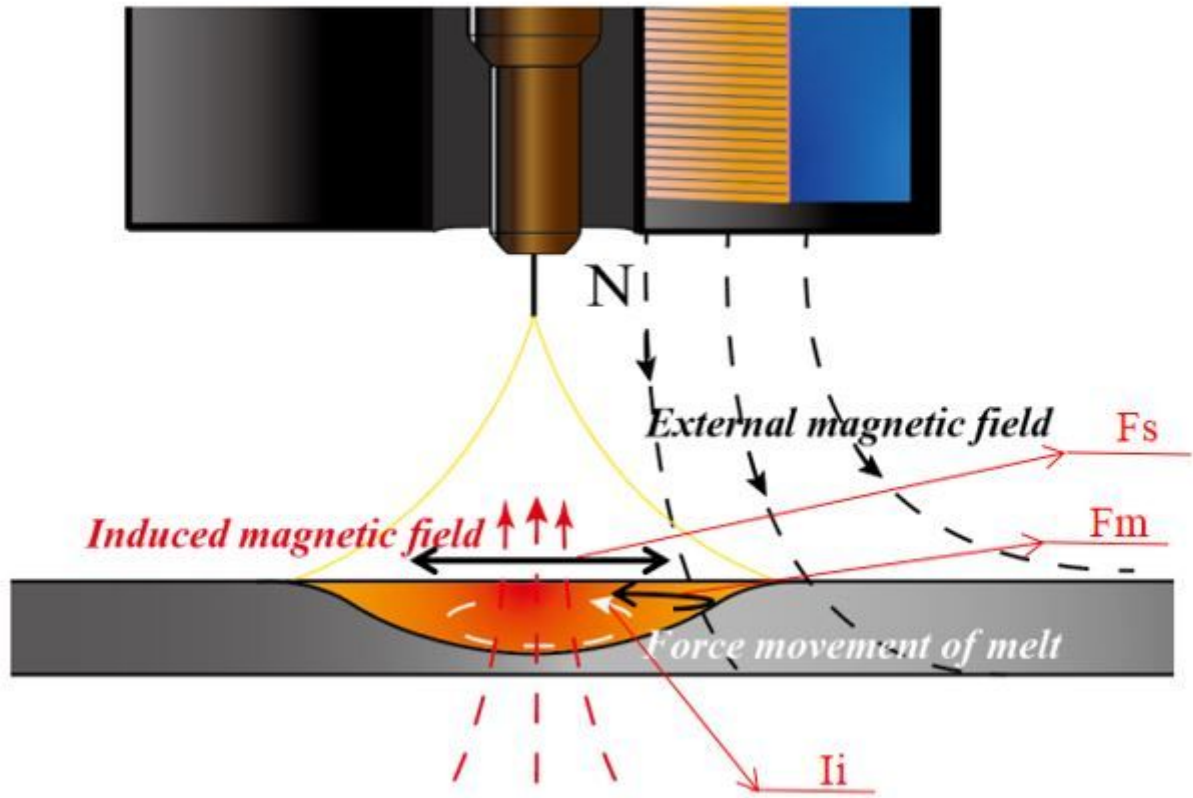


Figure 10

The melt produces an induced magnetic field under the external magnetic field